

# Tripletformer for Probabilistic Interpolation of Asynchronous Time Series

Vijaya Krishna Yalavarthi, Johannes Burchert, Lars Schmidt-Thieme

Information Systems and Machine Learning Lab  
University of Hildesheim

## Abstract

Asynchronous time series are often observed in several applications such as health care, astronomy, and climate science, and pose a significant challenge to the standard deep learning architectures. Interpolation of asynchronous time series is vital for many real-world tasks like root cause analysis, and medical diagnosis. In this paper, we propose a novel encoder-decoder architecture called Tripletformer, which works on the set of observations where each set element is a triple of time, channel, and value, for the probabilistic interpolation of the asynchronous time series. Both the encoder and the decoder of the Tripletformer are modeled using attention layers and fully connected layers, and are invariant to the order in which set elements are presented. The proposed Tripletformer is compared with a range of baselines over multiple real-world and synthetic asynchronous time series datasets, and the experimental results attest that it produces more accurate and certain interpolations. We observe an improvement in negative loglikelihood error up to 33% over real and 800% over synthetic asynchronous time series datasets compared to the state-of-the-art model by using the Tripletformer.

## 1 Introduction

In the domains like medical applications (Yadav et al. 2018), multivariate time series (MTS) are often observed asynchronously, meaning the variables (or sensors) are observed independent to each other, and we call such time series as Asynchronous Time Series (AsTS). Practitioners often want to determine the data that is not observed while data collection, but within the observed time range for a better analysis. As an example, a person being treated for some health issue missed a medical test. Later, a situation arises which makes the doctor think about the probable result of the missed test. An interpolation model can be used in order to obtain the probable value of the missed test result, and treat the patient in a better manner. In such situations, it is desired that interpolation models predict not only the observation measurement but also the uncertainty surrounding it such that overly confident values can be avoided.

Deep learning models are widely studied for the imputation tasks (Jäger, Allhorn, and Bießmann 2021) in general MTS with missing values where i) the time series is observed at regular intervals, ii) sparsity (number of missing values over the number of observed values) is small, iii) all

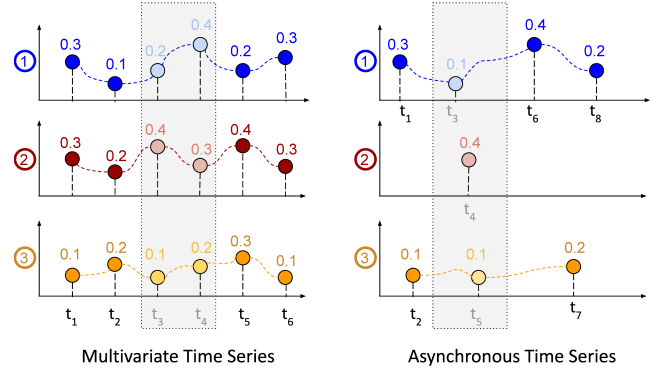


Figure 1: Interpolation in Multivariate Time Series (a) and Asynchronous Time Series (b). In (a) all the channels in the time series are observed at times  $t_1, t_2, t_5, t_6$  and we need to interpolate the values for all the channels at  $t_3, t_4$ . Where as in (b), channel 1 is observed at times  $t_1, t_6, t_8$ , and channel 3 is observed at  $t_2, t_7$ . We did not make any observation in channel 2. However, we need to interpolate the values for channels 1, 2 and 3 at time points  $t_3, t_4$ , and  $t_5$  respectively.

the channels are of equal lengths. On the contrary, AsTS often consist of i) non-periodic observations in a channel, ii) extremely sparse channels when one tries to align the AsTS iii) variable channel lengths in a single example, and iv) totally unobserved channels (missing entire channel). Because of these properties, modeling AsTS is often difficult for the standard deep learning models. In Figure 1, we delineate interpolation in AsTS from MTS.

While most of the existing literature concentrates on the classification of the AsTS (Shukla and Marlin 2021; Li and Marlin 2016; Rubanova, Chen, and Duvenaud 2019; Kidger et al. 2020; Horn et al. 2020; Shukla and Marlin 2019), a few works (Shukla and Marlin 2021; Chen et al. 2018; Rubanova, Chen, and Duvenaud 2019) study deterministic interpolation. Among them, multi Time Attention Network (mTAN) (Shukla and Marlin 2021) that uses Variational Autoencoder (VAE) based approach produces the state-of-the-art results for the deterministic interpolation. Recently, Sukla et. al. (Shukla and Marlin 2022) proposed Heteroscedastic Variational Autoencoder (HETVAE), a model that uses an Uncertainty aware multi Time Attention Network (UnTAN) and outputs heteroscedastic variance for

probabilistic interpolation in AsTS. Similar to mTAN, UnTAN converts the time series with variable channel lengths to fixed dimension using a time attention model. However, HETVAE struggles to learn the cross channel interactions because it utilizes a separate time attention model for each channel. We show through our experiments that encoding observations in all the channels using a single encoder is useful and produces better interpolations.

In this work, we propose a novel encoder-decoder architecture, that we call Tripletformer, made of attention layers and feed forward layers that are similar to Transformer model (Vaswani et al. 2017) for the probabilistic interpolation of AsTS. As the name suggests, our Tripletformer operates on the set of observations that are in triplet form (time, channel and value of the observation). We model time and channel as the independent variables, and the observation measurement (value) as the dependent variable. The encoder of the Tripletformer learns the interactions among the inter and intra channel observations of the AsTS simultaneously, while the decoder produces the probability distributions of the dependent variable over the set of reference (or target) independent variables. In order to overcome the computational complexity bottleneck of canonical attention and provide restricted attention mechanism for better learning, we use induced multi-head attention block (Lee et al. 2019) that has near linear computational complexity depending on the corresponding hyperparameter (that we explain in Section 3.4).

We evaluate the proposed Tripletformer over multiple real-world and synthetic AsTS datasets at varying observation levels, and two different missing patterns. The Tripletformer is compared with the state-of-the-art probabilistic interpolation model, HETVAE, and a range of baselines using Negative Loglikelihood loss (NLL) as the evaluation metric. Our experimental results attest that the proposed Tripletformer provides significantly better interpolations compared to its competitors.

Our contributions are summarized as follows:

- We propose a novel model called Tripletformer that can learn both inter and intra channel interactions simultaneously in the AsTS by operating on the set of observations for the problem of probabilistic interpolation.
- We employ induced multi-head attention in order to reduce the computational complexity, and learn restricted attention for the better predictions. To the best of our knowledge, we are the first to use induced multi-head attention for AsTS.
- We perform extensive experimental evaluation of AsTS on three real and two synthetic AsTS datasets, under two different missing patterns. Our experimental results attest that Tripletformer provides up to 33% and 800% improvement in NLL over real and synthetic AsTS datasets, respectively compared to the HETVAE.

We provide the source code for the Tripletformer in <https://github.com/yalavarthivk/tripletformer>

## 2 Related Work

The focus of this work is on probabilistic interpolation in asynchronous time series. We briefly discuss the recent

works in the next few paragraphs.

Researchers proposed various models that use Variational Autoencoders (VAE) and provide homoscedastic outputs. (Chen et al. 2018) proposed Neural Ordinary Differential Equations (ODE) network for modeling time series using a continuous time function in the hidden state. Later, (Rubanova, Chen, and Duvenaud 2019) proposed an architecture with ODE-RNN as the encoder which uses Neural ODE to model the latent state dynamics, and an RNN to update it when a new observation is made. (Li et al. 2020) proposed stochastic differential equations (SDEs), generalizing ODEs, defined using nonstandard integrals usually relying on Itô calculus. (Norcliffe et al. 2021) proposed Neural ODE processes (NDPs) by combining the Neural ODEs with Neural Process (Garnelo et al. 2018). NDPs are a class of stochastic processes that are determined by a distribution over Neural ODEs. (Shukla and Marlin 2021) proposed multi-Time Attention Networks (mTAN) that uses a temporal attention network at both encoder and decoder for producing the deterministic interpolations. mTAN provides the state-of-the-art results for deterministic interpolation.

While VAE based models produce homoscedastic variance; one can produce heteroscedastic variance by outputting the distribution parameters. Gaussian Process Regression (GPR) (Williams and Rasmussen 2006) provides full joint posterior distributions over interpolation outputs. GPR models can be directly implemented on AsTS by applying one model for each channel. On the other hand, GPRs can be used in multivariate setting but it requires a positive definite constraint on the co-variance matrix. (Shukla and Marlin 2022) show that the GPR that uses a single GP for channel provides better results compared to the GPR that works in multivariate setting (Bonilla, Chai, and Williams 2007) for AsTS. Finally, (Shukla and Marlin 2022) proposed HETVAE model which is the first work (and only work that is prior to us to the best of our knowledge) that deals with the problem of probabilistic interpolation in AsTS. It consists of an Uncertainty aware multi-Time Attention Networks (UnTAN) that uses a combination of probabilistic and deterministic paths to output heteroscedastic variance.

In our work, we use an attention based model for the probabilistic interpolation. Our model operates on a set of observations and produces heteroscedastic variance.

## 3 Background and Preliminaries

### 3.1 AsTS as set of observations

Our set representation of AsTS follows the representation provided in (Horn et al. 2020). Given an AsTS dataset  $\mathcal{X} = \{X^n\}_{n=1}^N$  of  $N$  many examples, an AsTS  $X^n$  can be formulated as set of observations  $x_i^n$  such that  $X^n = \{x_1^n, x_2^n, \dots, x_{|X^n|}^n\}$ . We omit superscript  $n$  when the context is clear. Each observation  $x_i$  is a triple consisting of time, channel and value (observation measurement),  $x_i = (t_i, c_i, u_i)$ , with  $t_i \in \mathcal{T} = \{\tau_1, \tau_2, \dots, \tau_{|\mathcal{T}|}\}$ ,  $\mathcal{T}$  being the set of all the observation times in the series  $X$ ,  $c_i \in \mathcal{C} = \{1, 2, 3, \dots, C\}$ ,  $\mathcal{C}$  being the set of channels in all the AsTS dataset  $\mathcal{X}$ . In Figure 2, we demonstrate the representation of

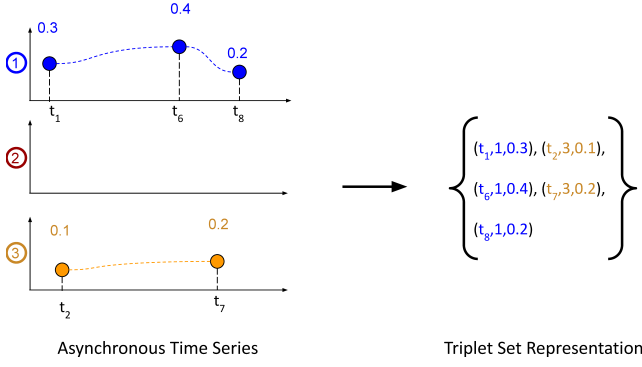


Figure 2: Demonstration of AsTS as set of observations.

AsTS as set of observations.

### 3.2 Probabilistic Interpolation of AsTS

In deterministic interpolation, one wants to estimate the most probable value of the dependent variable. While deterministic interpolation provides a single estimate, probabilistic interpolation outputs the probability distribution that explains the prediction’s uncertainty.

Given an asynchronous time series  $X \in \mathcal{X}$ , independent variables ( $w = (t', c')$ ) in the target observations that are time  $t' \notin \mathcal{T}$ ,  $\min(\mathcal{T}) < t' < \max(\mathcal{T})$ , channel indicator  $c' \in \mathcal{C}$ ; the goal is to predict the probability distribution of the dependent variable  $u'$  i.e., find  $\hat{Pr}(u'|X, w)$ .

### 3.3 Multihead Attention Block (MAB)

MAB (Vaswani et al. 2017; Lee et al. 2019) consists of two sublayers: i) Multihead Attention (MHA) (Vaswani et al. 2017), and ii) a pointwise feed forward layer (MLP) as shown in Figure 3(a). We have a residual connection around both the sublayers.

$$\begin{aligned} \text{MAB}(q, k, v) &= \alpha(H + \text{MLP}(H)) \\ \text{where } H &= \alpha(q + \text{MHA}(q, k, v)) \end{aligned} \quad (1)$$

with  $q, k, v$  being query, key and value sequences and,  $\alpha$  is a non-linear activation function.

In MHA, the attention matrix ( $A$ ) which requires the multiplication of  $L_q \times d$  and  $L_k \times d$  sized matrices has a computational complexity of  $\mathcal{O}(L_q L_k d)$ .  $L_q, L_k, d$  are the query length, key length and embedding dimensions respectively. When both  $L_q$  and  $L_k$  are large, computing  $A$  will be a bottleneck because of its quadratic computational complexity.

### 3.4 Induced Multihead Attention Block (IMAB)

Because computing  $A$  in MHA is infeasible for long sequences, (Lee et al. 2019) proposed the Induced Multihead Attention Block (IMAB) that consists of two MABs and  $l$  many  $d_h$  dimensional induced points  $h \in \mathbb{R}^{l \times d_h}$  which are trainable parameters. An IMAB can be given as:

$$\begin{aligned} \text{IMAB}(q, k, v) &= \text{MAB}(q, \mathcal{H}, \mathcal{H}) \\ \text{where } \mathcal{H} &= \text{MAB}(h, k, v) \end{aligned} \quad (2)$$

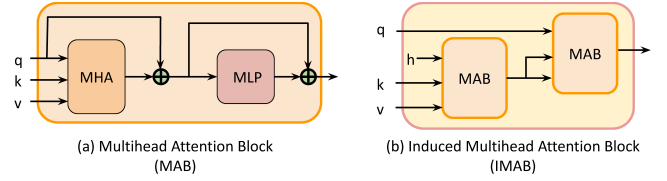


Figure 3: Architectures of Multihead Attention Block (a) and Induced Multihead Attention Block (b) (Lee et al. 2019)

The architecture of IMAB is shown in Figure 3(b). The computational complexity of the IMAB is  $\mathcal{O}(L_q l d + L_k l d)$  which is near linear when  $l \ll L_q, L_k$ .

IMAB is the optimal choice of model because i) it reduces the computational complexity and ii) provides learned restricted attention phenomena. Probsparse attention (Zhou et al. 2021) which provides restricted attention is the state-of-the-art model used in time series forecasting. It ranks the key tokens by their impact on the query, and restricts its attention to the top- $K$  tokens only rather than the entire key set. It was shown that using restricted attention provides similar or better results compared to the canonical attention (see (Zhou et al. 2021) for more details). However, the main drawback of Probsparse attention is, it assumes the lengths of all the series in a batch are equal which is not the case while working with AsTS. In order to have a consistent batch, we pad the series of smaller lengths with zeros, and the sparse attentions treat observations and zero padding in the same manner for sampling the important key tokens which is incorrect. On the other hand, when we are operating on sets, it is not trivial to find the key tokens that are important to the query, manually. Hence, one can learn a set of clusters called reference clusters ( $\mathcal{H}$  in equation 2) using  $h$  that act as basis for the restriction. Then, the queries attend to those reference clusters rather than the entire key set.

## 4 Proposed Model: Tripletformer

Our proposed Tripletformer holds an encoder-decoder architecture for the problem of probabilistic interpolation in AsTS. It leverages on the asynchronous sampling of observations, and operates on the observations directly.

Our encoder  $E$ , similar to that of the transformer model (Vaswani et al. 2017), maps the input time series  $X$  which is a set of  $s = |X|$  many observations  $\{x_1, \dots, x_s\}$  to a set of continuous representations  $Z^{(e)} = \{z_1^{(e)}, \dots, z_s^{(e)}\}$  corresponding to  $X$ . Our decoder outputs the parameters of the probability distribution of the target observation value  $\hat{Pr}(u'|Z^{(e)}, w)$  conditioning up on the encoder output  $Z^{(e)}$ , and independent variables  $w = (t', c')$  of the target observation  $x'$ . The architecture of the proposed model is shown in Figure 4. We explain the encoder and decoder blocks in the following sections.

### 4.1 Encoder

Our encoder consists of i) an input embedding layer ( $iFF$ ) and ii) a Self-attention layer ( $SA$ ) which is an IMAB.

Our  $iFF$  is a point wise feed forward layer that provides learned embeddings to the set elements. Because our  $iFF$

works only on the vectors, we convert  $x \in X$  into a vector  $x \in \mathbb{R}^{C+2}$  by concatenating the time, channel indicator and value of the observation. We use one-hot encoding of the channel as its indicator.  $iFF$  takes  $X$  as input, and outputs its embeddings  $Y^{(e)} = \{y_1^{(e)}, \dots, y_s^{(e)}\}$ . These input embeddings are passed through Self-attention layer  $SA$  that consists of  $L$  many Induced Multihead Attention Blocks to produce latent embeddings  $Z^{(e)} = \{z_1^{(e)}, \dots, z_s^{(e)}\}$ .

Employing attention mechanism is a principled approach for the interpolation problem in AsTS. In AsTS, the length of a series (size of the set) varies, and we need a model that does not depend on the length of the series in order to learn the latent embeddings. For this, we can sort the set elements over time, and apply a Convolutional (CNN) or Recurrent Neural Networks (RNN). Although CNNs and RNNs are highly researched for the classification and forecasting tasks, they are not useful for interpolation tasks as the query time point is in between the observation times where convolution (or RNN) is already applied. Hence, the attention mechanism is a better choice as each observation attends to every other observation in the set. Also, the attention mechanism is permutation invariant which helps in applying them to sets.

## 4.2 Decoder

Our decoder takes the encoder output  $Z^{(e)}$ , set of  $r$  many target queries  $\{W = w_1, \dots, w_r\}$  as inputs, and outputs the distribution parameters of the target values  $\{U' = u'_1, \dots, u'_r\}$ .  $M = \{\mu_1, \dots, \mu_r\}$ , and  $\Sigma = \{\sigma_1, \dots, \sigma_r\}$  are the corresponding distribution parameters (mean and standard deviation assuming the underlying distribution as Gaussian) of  $W$ .

Our decoder consists of i) target embedding layer ( $tFF$ ), ii) Cross-attention block ( $CA$ ) and iii) output layer ( $O$ ).

Our target embedding layer  $tFF$  is a point wise feed forward layer that provides latent representation to the learned embedding of the target query. For a target query  $w \in W$ , we concatenate the time  $t'$  and channel indicator  $c'$  (one hot encoding), and get  $w \in \mathbb{R}^{C+1}$ . We pass  $W = \{w_1, \dots, w_r\}$  through  $tFF$  to obtain their latent representation  $Y^{(d)} = \{y_1^{(d)}, \dots, y_r^{(d)}\}$ . Our Cross-attention layer ( $CA$ ) takes the  $Y^{(d)}$  as query, and  $Z^{(e)}$  as keys and values for a MAB, and outputs the learned embeddings  $Z^{(d)} = \{z_1^{(d)}, \dots, z_r^{(d)}\}$ . Finally,  $Z^{(d)}$  is passed through the output layer  $O$  which is a feed forward layer with two output heads. The output layer produces the distribution parameters  $M$  and  $\Sigma$  corresponding to the elements present in  $W$ . We assume for a predictor  $w \in W$ ,  $\hat{Pr}(u'|X, w)$  defines the final probability distribution of  $u'$  (target observation value) with  $\hat{Pr}(u'|X, w) = \mathcal{N}(u'; \mu, \sigma)$ .

The following equations describe the flow of data in the model.  $E_\Lambda$  indicates embedding dimension of layer  $\Lambda$  with  $\Lambda \in \{iFF, SA, tFF, CA\}$ .

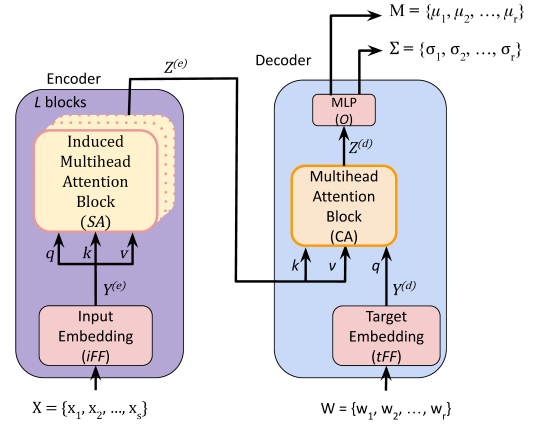


Figure 4: Tripletformer architecture. Encoder (left) takes the set of observations  $X$ , and output their embeddings  $Z^{(e)}$ . Decoder (right) takes  $Z^{(e)}$ , target queries ( $W$ ), and produces the mean  $M$  and standard deviation  $\Sigma$  corresponding to  $W$ .

$$iFF : X \mapsto Y^{(e)} \quad (\in \mathbb{R}^{s \times E_{iFF}}) \quad (3)$$

$$SA : Y^{(e)} \mapsto Z^{(e)} \quad (\in \mathbb{R}^{s \times E_{SA}}) \quad (4)$$

$$tFF : W \mapsto Y^{(d)} \quad (\in \mathbb{R}^{r \times E_{tFF}}) \quad (5)$$

$$CA : Y^{(d)}, Z^{(e)} \mapsto Z^{(d)} \quad (\in \mathbb{R}^{r \times E_{CA}}) \quad (6)$$

$$O : Z^{(d)} \mapsto M, \Sigma \quad (\in \mathbb{R}^r, \mathbb{R}_+^r) \quad (7)$$

$$u' \sim \hat{Pr}(u'|X, w) = \mathcal{N}(u'; \mu, \sigma), \quad (8)$$

$$\text{where } w = (t', c') \in W, \quad \mu \in M, \quad \sigma \in \Sigma$$

In various transformer like models (Vaswani et al. 2017; Zhou et al. 2021) that are used for time series forecasting, the decoder consists of a (masked or causal) Self-attention layer on the target query embeddings. This step consists of a transductive bias among the independent variables (covariates). In this work, we do not have covariates other than the time and channel of the observations. Hence, we do not require Self-attention among the target queries. Also, it is not necessary to apply any positional embeddings (Vaswani et al. 2017) to both encoder and decoder inputs because, our triplet already consists of time and channel information which act as a natural positional embedding of the observation. Further, because we use attention and position wise feed forward layers which do not depend on the location of the observation in the sequence (Lee et al. 2019), we say that our Tripletformer is invariant to the order in which set elements are presented to it.

In the proposed Tripletformer, we use IMAB in encoder and MAB in the decoder. Although IMAB can be used for both Self-attention (in the encoder) and Cross-attention (in the decoder), we observed that using IMAB for Cross-attention is not providing consistent advantage over MAB in terms of prediction accuracy (see Supp. material).

## 4.3 Supervised learning

Our Tripletformer works in a heteroscedastic manner outputting probability distribution for each query. We assume

that the data is following a Gaussian distribution, and use NLL as the main loss for training the model. In addition to NLL, we also use mean square error as the augmented loss in order to avoid the model sticking in local optima when the mean is almost flat after a few iterations. We optimize the following loss function  $\mathcal{L}$ :

$$\mathcal{L} = \sum_{n=1}^N -\mathbb{E}[\log \hat{P}_r(U'^n | X^n, W^n)] + \lambda \mathbb{E} \|U'^n - M^n\|_2^2$$

with  $\hat{P}_r(U'^n | X^n, W^n) = \prod_{j=1}^{r^n} \hat{P}_r(u_j^n | X^n, w_j^n)$  (9)

## 5 Experiments

### 5.1 Datasets

We experimented the proposed Tripletransformer on three real world AsTS datasets: Physionet2012 (Silva et al. 2012; Goldberger et al. 2000), MIMIC-III (Johnson et al. 2016; Harutyunyan et al. 2019) and Physionet2019 (Reyna et al. 2019) datasets. We also created two synthetic AsTS datasets from real world MTS namely PenDigits and PhonemeSpectra (Ruiz et al. 2021) (see Section 5.6).

### 5.2 Competing Models

Our Tripletransformer competes with the following models.

First, we compare with deterministic models that were made probabilistic by adding a homoscedastic variance which is a hyperparameter searched on the validation dataset. **Mean Imputation** always predicts the mean value of the channel in the training dataset. **Forward Imputation** predicts the value of the previous observation in the channel. If there is no value observed in that particular channel, which is usual for AsTS, we impute with zero. **L-ODE-RNN** (Chen et al. 2018) is a Neural Ordinary Different Equation (ODE) model where the decoder is an ODE-RNN while the encoder is made of an RNN. **L-ODE-ODE** (Rubanova, Chen, and Duvenaud 2019) is also an ODE model where the encoder consists of an ODE-RNN instead of an RNN. **mTAN** (Shukla and Marlin 2021), Multi-Time attention Network is the state-of-the-art deterministic interpolation model that uses time attention networks for the series encoding and decoding.

We also compare with the following heteroscedastic models. **GPR** (Williams and Rasmussen 2006) is the Gaussian Process regression modality where one model is trained per channel. **HETVAE** (Shukla and Marlin 2022), Heteroscedastic Temporal Variational Autoencoder for Irregular Time Series (HETVAE) is the state-of-the-art probabilistic interpolation model for Asynchronous time series. *To the best of our knowledge, this is the only work, prior to ours, that deals with the problem of probabilistic interpolation.*

### 5.3 Experimental Setup

We randomly split each dataset into train and test with 80% and 20% samples, and 20% of the train data for validation.

We search the following hyperparameters:  $L \in \{1, 2, 3, 4\}$ , hidden units in MLP layers (feed forward layers

Table 1: Results of **observations missing at random** on real AsTS datasets. Evaluation measure is NLL, lower the best.

	Observed %	10%	50%	90%
Physionet 2012	Mean	1.406	1.406	1.402
	Forward	1.371	1.217	1.164
	GPR	0.956±0.001	0.767±0.006	0.798±0.004
	L-ODE-RNN	1.268±0.012	1.233±0.027	1.280±0.029
	L-ODE-ODE	1.211±0.001	1.168±0.001	1.170±0.003
	mTAN	1.110±0.000	0.934±0.001	0.923±0.002
	HETVAE	0.849±0.008	0.578±0.005	0.551±0.011
	Tripletransformer	<b>0.780±0.013</b>	<b>0.455±0.011</b>	<b>0.373±0.040</b>
MIMIC-III	Mean	1.508	1.508	1.507
	Forward	1.750	1.423	1.328
	GPR	1.201±0.003	0.979±0.006	0.919±0.000
	mTAN	1.209±0.000	1.066±0.001	1.065±0.001
	HETVAE	1.077±0.003	0.828±0.001	0.774±0.008
	Tripletransformer	<b>1.056±0.006</b>	<b>0.789±0.006</b>	<b>0.710±0.010</b>
Physionet 2019	Mean	1.421	1.420	1.425
	Forward	1.361	1.205	1.433
	GPR	1.136±0.000	0.907±0.012	0.851±0.007
	mTAN	1.152±0.001	0.988±0.002	0.982±0.006
	HETVAE	1.091±0.001	0.855±0.002	0.835±0.005
	Tripletransformer	<b>1.079±0.001</b>	<b>0.806±0.004</b>	<b>0.752±0.007</b>

in both encoder and decoder) from  $\{64, 128, 256\}$ , attention layers dimension from  $\{64, 128, 256\}$ , number of induced points in IMAB from  $\{16, 32, 64, 128\}$ , and  $\lambda$  augmented loss weight from  $\{0, 1, 5, 10\}$ . Similar to (Horn et al. 2020), we trained all the competing models for 5 different random hyperparameter setups, and chose the one that has the least NLL on the validation dataset. We independently run the experiments for 5 times using the best hyperparameters and different random seeds. The best hyperparameters for all the competing models are provided in the supplementary material. We code all the models using PyTorch, and trained on NVIDIA GeForce RTX 3090 GPUs.

### 5.4 Sampling techniques

In the experiments, we considered two types of setups for sampling  $X$  (observations on which interpolations are conditioned) for the interpolation task.

**Random missing:** In this setup, we assume that the sensors are missed at random time points. Hence we condition on the random time points and predict the observation values of all the available channels for the remaining time points.

**Burst missing:** Here, we assume that the sensors are not observed for a series of time points. We randomly choose a start time point, and use  $p$  many time points after that for prediction by conditioning upon the remaining.

### 5.5 Results on real AsTS datasets

Our main experimental results using two different sampling techniques on real AsTS datasets are presented below.

**Results on random sampling:** In Table 1, we present the results for the random sampling technique. We use three different conditioning ranges (tp.obs) which are 10%, 50% and 90% of all the observations in the series. We were not able to run ODE models on MIMIC-III and Physionet2019 datasets



Table 2: Results of **bursts of observations missing** on real AsTS datasets. Evaluation measure is NLL, lower the best.

	Observed %	10%	50%	90%
Physionet 2012	Mean	1.412	1.382	1.407
	Forward	1.534	1.442	1.232
	GPR	1.127 $\pm$ 0.018	0.983 $\pm$ 0.002	0.691 $\pm$ 0.001
	L-ODE-RNN	1.270 $\pm$ 0.002	1.382 $\pm$ 0.006	1.289 $\pm$ 0.011
	L-ODE-ODE	1.263 $\pm$ 0.000	1.242 $\pm$ 0.002	1.243 $\pm$ 0.001
	mTAN	1.200 $\pm$ 0.000	1.141 $\pm$ 0.001	0.960 $\pm$ 0.001
	HETVAE	1.028 $\pm$ 0.011	0.882 $\pm$ 0.002	0.614 $\pm$ 0.039
	Tripletformer	<b>0.925<math>\pm</math>0.005</b>	<b>0.777<math>\pm</math>0.013</b>	<b>0.578<math>\pm</math>0.034</b>
MIMIC-III	Mean	1.509	1.507	1.515
	Forward	1.870	1.608	1.412
	GPR	1.328 $\pm$ 0.000	1.231 $\pm$ 0.004	1.000 $\pm$ 0.039
	mTAN	1.319 $\pm$ 0.001	1.247 $\pm$ 0.000	1.094 $\pm$ 0.002
	HETVAE	1.210 $\pm$ 0.000	1.126 $\pm$ 0.003	0.939 $\pm$ 0.009
	Tripletformer	<b>1.193<math>\pm</math>0.003</b>	<b>1.087<math>\pm</math>0.006</b>	<b>0.885<math>\pm</math>0.032</b>
Physionet 2019	Mean	1.425	1.415	1.419
	Forward	1.466	1.368	1.209
	GPR	1.257 $\pm$ 0.001	1.049 $\pm$ 0.002	0.975 $\pm$ 0.005
	mTAN	1.269 $\pm$ 0.001	1.113 $\pm$ 0.001	1.042 $\pm$ 0.002
	HETVAE	1.241 $\pm$ 0.001	1.012 $\pm$ 0.004	0.949 $\pm$ 0.002
	Tripletformer	<b>1.222<math>\pm</math>0.001</b>	<b>0.977<math>\pm</math>0.005</b>	<b>0.865<math>\pm</math>0.009</b>

because of the high computational requirement. However, for the datasets we evaluated, ODE models performed significantly worse than Tripletformer. Hence, it is safe to assume that ODE models perform worse in the remaining datasets as well. We see that our Tripletformer outperforms all the competing models with a huge margin. Especially, we see significant lifts with the Physionet2012 dataset compared to the next best model, HETVAE. As an example, when we condition on 90% of the times, we achieve an improvement of 33% in the NLL.

We note that the published results (Shukla and Marlin 2022) with 50% time points in conditioning range using random missing for both the Physionet2012 and MIMIC-III differ from ours. For the Physionet2012, this can be attributed to the following: 1) in (Shukla and Marlin 2022), the dataset was normalized using the parameters computed on the entire dataset instead of training dataset, 2) inclusion of erroneous observations in (Shukla and Marlin 2022) (see suppl. material). Also, we were not able to reproduce the results with the preprocessing details provided in (Shukla and Marlin 2022). Whereas, for MIMIC-III dataset, we could not extract the splits used in (Shukla and Marlin 2022), hence used another standard version (Horn et al. 2020; Harutyunyan et al. 2019).

**Results on burst sampling:** We present the results for burst sampling in Table 2. Interpolating the burst missing values is a difficult task compared to that of random missing. Because, in burst missing, conditioning time points are far from the query time point whereas in random sampling they are close by. The results on burst sampling show a similar pattern to random sampling. Our Tripletformer outperforms all the models with a significant margin; HETVAE and GPR are the second and third best models. We see significant lifts in this setup as well compared to the state-of-the-art model,

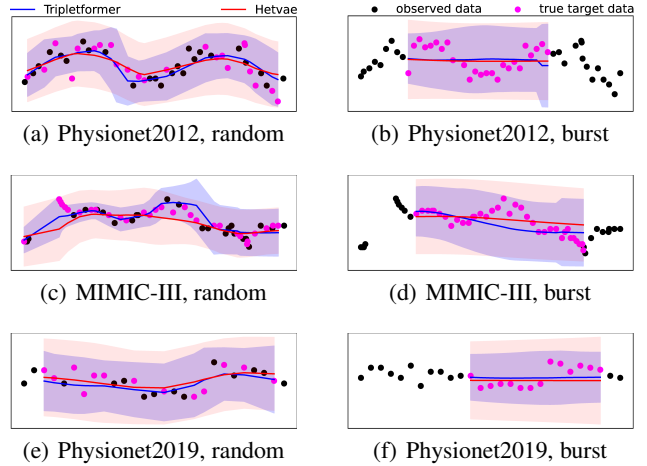


Figure 5: Comparison of qualitative performance between Tripletformer and HETVAE. Plots are the predictions (95<sup>th</sup> quantile) of both the models for heart rate in all the three datasets conditioned on the 50% of the time points.

HETVAE. Again, in Physionet2012 dataset with 50% of the observations in the conditioning range, our Tripletformer has around 12% improvement in NLL.

We perform a qualitative comparison of the predictions made by the Tripletformer and HETVAE models in Figure 5. We observe that the Tripletformer provides not only accurate predictions but also with higher certainty which is desirable in probabilistic interpolation.

## 5.6 Experiments with synthetic AsTS datasets

Here, we impose synthetic AsTS setup on real world MTS. Because in AsTS sensors are observed asynchronously and independently, we assume that at every point of time only one sensor is observed. Hence, from MTS, we randomly chose one variable at a single point of time, and remove all the remaining variables making the number of observations in synthetic AsTS is same as the length of the source MTS.

For this, we choose PenDigits and PhonemeSpectra datasets which are the second and third largest datasets used in (Ruiz et al. 2021). Although FaceDetection is the largest dataset, it does not show any variance in the interpolation results across models, across sampling rates and sampling techniques. Hence, we use the next best dataset available. Experimental results for random and burst sampling are presented in Tables 3 and 4. Because PenDigits has short time series (series length = 8), burst sampling and random sampling gives same observations in the conditioning and target ranges when 90% of the series is observed, hence, we get same results for both sampling techniques. It can be observed that for both the sampling types, and all the conditioning ranges, Tripletformer outperforms all the other competing models with a significant margin. Especially, for PhonemeSpectra, random sampling and conditioning range of 90%, Tripletformer produces 800% better predictions compared to HETVAE.

The reason for the poor performance of the HETVAE on

Table 3: Results of synthetic AsTS for **observations missing at random**. Evaluation measure is NLL, lower the best.

	Observed %	10%	50%	90%
Pen Digits	Mean	1.424	1.420	1.424
	Forward	1.550	1.626	1.596
	GPR	1.411 $\pm$ 0.001	1.350 $\pm$ 0.030	1.279 $\pm$ 0.055
	L-ODE-RNN	1.285 $\pm$ 0.005	1.183 $\pm$ 0.012	1.102 $\pm$ 0.014
	L-ODE-ODE	1.307 $\pm$ 0.001	1.182 $\pm$ 0.002	1.108 $\pm$ 0.004
	mTAN	1.307 $\pm$ 0.001	1.050 $\pm$ 0.013	0.882 $\pm$ 0.020
	HETVAE	1.267 $\pm$ 0.003	1.207 $\pm$ 0.025	1.326 $\pm$ 0.015
	Tripletformer	<b>1.115<math>\pm</math>0.003</b>	<b>0.693<math>\pm</math>0.019</b>	<b>0.463<math>\pm</math>0.027</b>
Phoneme Spectra	Mean	1.437	1.437	1.435
	Forward	1.553	1.559	1.528
	GPR	1.378 $\pm$ 0.002	1.271 $\pm$ 0.005	1.176 $\pm$ 0.009
	L-ODE-RNN	1.327 $\pm$ 0.006	1.289 $\pm$ 0.010	1.263 $\pm$ 0.025
	L-ODE-ODE	1.304 $\pm$ 0.002	1.273 $\pm$ 0.006	1.264 $\pm$ 0.008
	mTAN	1.225 $\pm$ 0.003	0.963 $\pm$ 0.009	1.097 $\pm$ 0.010
	HETVAE	1.033 $\pm$ 0.031	0.699 $\pm$ 0.004	0.804 $\pm$ 0.002
	Tripletformer	<b>0.923<math>\pm</math>0.008</b>	<b>0.413<math>\pm</math>0.005</b>	<b>0.115<math>\pm</math>0.024</b>

Table 4: Results of synthetic AsTS for **observations missing at burst**. Evaluation measure is NLL, lower the best.

	Observed %	10%	50%	90%
Pen Digits	Mean	1.427	1.396	1.424
	Forward	1.556	1.683	1.596
	GPR	1.386 $\pm$ 0.006	1.413 $\pm$ 0.000	1.279 $\pm$ 0.055
	L-ODE-RNN	1.271 $\pm$ 0.002	1.184 $\pm$ 0.005	1.144 $\pm$ 0.007
	L-ODE-ODE	1.269 $\pm$ 0.002	1.207 $\pm$ 0.020	1.171 $\pm$ 0.075
	mTAN	1.277 $\pm$ 0.002	1.061 $\pm$ 0.004	0.882 $\pm$ 0.023
	HETVAE	1.270 $\pm$ 0.001	1.188 $\pm$ 0.006	1.326 $\pm$ 0.033
	Tripletformer	<b>1.115<math>\pm</math>0.000</b>	<b>0.787<math>\pm</math>0.015</b>	<b>0.463<math>\pm</math>0.027</b>
Phoneme Spectra	Mean	1.441	1.436	1.456
	Forward	1.583	1.643	1.610
	GPR	1.387 $\pm$ 0.000	1.331 $\pm$ 0.000	1.309 $\pm$ 0.001
	L-ODE-RNN	1.389 $\pm$ 0.010	1.356 $\pm$ 0.013	1.309 $\pm$ 0.002
	L-ODE-ODE	1.367 $\pm$ 0.001	1.343 $\pm$ 0.002	1.290 $\pm$ 0.001
	mTAN	1.350 $\pm$ 0.001	1.285 $\pm$ 0.001	1.314 $\pm$ 0.008
	HETVAE	1.237 $\pm$ 0.003	1.057 $\pm$ 0.002	1.006 $\pm$ 0.002
	Tripletformer	<b>1.180<math>\pm</math>0.008</b>	<b>1.025<math>\pm</math>0.005</b>	<b>0.975<math>\pm</math>0.009</b>

synthetic datasets is the encoding of each channel separately. We observe that the medical datasets do not have significant cross channel interactions compared to the synthetic AsTS datasets making HETVAE shine comparatively better in the former. However, *for both synthetic and real AsTS datasets, Tripletformer outperforms HETVAE significantly.*

## 5.7 Experiment on Deterministic Interpolation

Here, we demonstrate the performance of the Tripletformer for deterministic interpolation. We trained both Tripletformer and HETVAE for predicting the mean value (optimized for Mean Squared Error loss). We compare the Tripletformer with HETVAE (Shukla and Marlin 2022) (probabilistic model), mTAN (Shukla and Marlin 2021), L-ODE-ODE (Rubanova, Chen, and Duvenaud 2019) and L-ODE-RNN (Chen et al. 2018) models over the published results (Shukla and Marlin 2021) on Physionet2012 dataset for random sampling in Table 5. We run the experiments on the dataset splits provided by (Shukla and Marlin 2021). We

Table 5: Comparison of competing models for deterministic interpolation on Physionet2012 dataset and random missing. Evaluation metric Mean Squared Error, lower the best.

Model	Mean Squared Error ( $\times 10^{-3}$ )			
L-ODE-RNN	8.132 $\pm$ 0.020	8.171 $\pm$ 0.030	8.402 $\pm$ 0.022	
L-ODE-ODE	6.721 $\pm$ 0.109	6.798 $\pm$ 0.143	7.142 $\pm$ 0.066	
mTAN	4.139 $\pm$ 0.029	4.157 $\pm$ 0.053	4.798 $\pm$ 0.036	
HETVAE	4.200 $\pm$ 0.500	4.945 $\pm$ 0.000	4.600 $\pm$ 0.000	
Tripletformer	<b>3.500<math>\pm</math>0.100</b>	<b>3.600<math>\pm</math>0.100</b>	<b>3.900<math>\pm</math>0.200</b>	
Observed %	50%	70%	90%	

Table 6: Comparing Tripletformer and Tf-enc-MAB. Tf-enc-MAB is a variant of Tripletformer and consists of the MAB in the encoder instead of the IMAB. Results of synthetic AsTS. Evaluation measure is NLL, lower the best.

	tp. obs.	10%	50%	90%
random sampling				
Pen	Tf-enc-MAB	1.117 $\pm$ 0.001	0.713 $\pm$ 0.009	0.551 $\pm$ 0.026
Digits	Tripletformer	<b>1.115<math>\pm</math>0.003</b>	<b>0.693<math>\pm</math>0.019</b>	<b>0.463<math>\pm</math>0.027</b>
Phoneme	Tf-enc-MAB	0.966 $\pm$ 0.010	0.626 $\pm$ 0.142	0.504 $\pm$ 0.156
Spectra	Tripletformer	<b>0.923<math>\pm</math>0.008</b>	<b>0.413<math>\pm</math>0.005</b>	<b>0.115<math>\pm</math>0.024</b>
burst sampling				
Pen	Tf-enc-MAB	1.111 $\pm$ 0.002	0.838 $\pm$ 0.020	0.551 $\pm$ 0.026
Digits	Tripletformer	<b>1.115<math>\pm</math>0.000</b>	<b>0.787<math>\pm</math>0.015</b>	<b>0.463<math>\pm</math>0.027</b>
Phoneme	Tf-enc-MAB	1.205 $\pm$ 0.009	1.035 $\pm$ 0.004	1.019 $\pm$ 0.026
Spectra	Tripletformer	<b>1.180<math>\pm</math>0.008</b>	<b>1.025<math>\pm</math>0.005</b>	<b>0.975<math>\pm</math>0.009</b>

observe that the Tripletformer outperforms all the models with a significant margin for deterministic interpolation as well.

## 5.8 Ablation Study:

In table 6, we compare the performance of Tripletformer with its variant Tf-enc-MAB which consists of MAB in the encoder. We use synthetic AsTS datasets for comparison because we could not run Tf-enc-MAB on all the splits of real AsTS datasets.

We see that choosing IMAB instead of MAB in the encoder is optimal. As mentioned in Section 3.4, Tripletformer that has IMAB in the encoder provides similar or better performance compared to Tf-enc-MAB demonstrating the advantage of restricted attention in IMAB. We see significant lifts when conditioning range increases from 10% to 90%.

## Conclusions

In this work, we propose a novel model called Tripletformer for the problem of probabilistic interpolation in Asynchronous Time Series. Our Tripleformer consists of a transformer like architecture, operates on a set of observations. We employ induced multi-head attention block in the encoder in order to learn the restricted attention mechanism, and to circumvent the problem of quadratic computational complexity of the canonical attention. We experimented on multiple real and synthetic asynchronous datasets, various conditioning ranges and two different sampling techniques. Our experimental results attest that the proposed Tripletformer provides better interpolations compared to the state-

of-the-art model HETVAE.

## References

- Bonilla, E. V.; Chai, K.; and Williams, C. 2007. Multi-task Gaussian process prediction. *Advances in neural information processing systems*, 20.
- Chen, R. T.; Rubanova, Y.; Bettencourt, J.; and Duvenaud, D. 2018. Neural ordinary differential equations. *arXiv preprint arXiv:1806.07366*.
- Garnelo, M.; Schwarz, J.; Rosenbaum, D.; Viola, F.; Rezende, D. J.; Eslami, S.; and Teh, Y. W. 2018. Neural processes. *arXiv preprint arXiv:1807.01622*.
- Goldberger, A. L.; Amaral, L. A.; Glass, L.; Hausdorff, J. M.; Ivanov, P. C.; Mark, R. G.; Mietus, J. E.; Moody, G. B.; Peng, C.-K.; and Stanley, H. E. 2000. PhysioBank, PhysioToolkit, and PhysioNet: components of a new research resource for complex physiologic signals. *circulation*, 101(23): e215–e220.
- Harutyunyan, H.; Khachatrian, H.; Kale, D. C.; Ver Steeg, G.; and Galstyan, A. 2019. Multitask learning and benchmarking with clinical time series data. *Scientific data*, 6(1): 1–18.
- Horn, M.; Moor, M.; Bock, C.; Rieck, B.; and Borgwardt, K. 2020. Set functions for time series. In *International Conference on Machine Learning*, 4353–4363. PMLR.
- Jäger, S.; Allhorn, A.; and Bießmann, F. 2021. A benchmark for data imputation methods. *Frontiers in big Data*, 48.
- Johnson, A. E.; Pollard, T. J.; Shen, L.; Li-Wei, H. L.; Feng, M.; Ghassemi, M.; Moody, B.; Szolovits, P.; Celi, L. A.; and Mark, R. G. 2016. MIMIC-III, a freely accessible critical care database. *Scientific data*, 3(1): 1–9.
- Kidger, P.; Morrill, J.; Foster, J.; and Lyons, T. 2020. Neural controlled differential equations for irregular time series. *arXiv preprint arXiv:2005.08926*.
- Lee, J.; Lee, Y.; Kim, J.; Kosiorek, A.; Choi, S.; and Teh, Y. W. 2019. Set transformer: A framework for attention-based permutation-invariant neural networks. In *International conference on machine learning*, 3744–3753. PMLR.
- Li, S. C.-X.; and Marlin, B. 2016. A scalable end-to-end gaussian process adapter for irregularly sampled time series classification. *Advances in Neural Information Processing Systems* 29.
- Li, X.; Wong, T.-K. L.; Chen, R. T.; and Duvenaud, D. 2020. Scalable gradients for stochastic differential equations. In *International Conference on Artificial Intelligence and Statistics*, 3870–3882. PMLR.
- Norcliffe, A.; Bodnar, C.; Day, B.; Moss, J.; and Liò, P. 2021. Neural ode processes. *9th International Conference on Learning Representations, ICLR*.
- Reyna, M. A.; Josef, C.; Seyedi, S.; Jeter, R.; Shashikumar, S. P.; Westover, M. B.; Sharma, A.; Nemati, S.; and Clifford, G. D. 2019. Early prediction of sepsis from clinical data: the PhysioNet/Computing in Cardiology Challenge 2019. In *2019 Computing in Cardiology (CinC)*, Page–1. IEEE.
- Rubanova, Y.; Chen, R. T.; and Duvenaud, D. 2019. Latent odes for irregularly-sampled time series. *Advances in Neural Information Processing Systems* 32.
- Ruiz, A. P.; Flynn, M.; Large, J.; Middlehurst, M.; and Bagnall, A. 2021. The great multivariate time series classification bake off: a review and experimental evaluation of recent algorithmic advances. *Data Mining and Knowledge Discovery*, 35(2): 401–449.
- Shukla, S. N.; and Marlin, B. 2021. Multi-Time Attention Networks for Irregularly Sampled Time Series. In *International Conference on Learning Representations*.
- Shukla, S. N.; and Marlin, B. M. 2019. Interpolation-prediction networks for irregularly sampled time series. *International Conference on Learning Representations*.
- Shukla, S. N.; and Marlin, B. M. 2022. Heteroscedastic Temporal Variational Autoencoder For Irregularly Sampled Time Series. *International Conference on Learning Representation*.
- Silva, I.; Moody, G.; Scott, D. J.; Celi, L. A.; and Mark, R. G. 2012. Predicting in-hospital mortality of icu patients: The physionet/computing in cardiology challenge 2012. In *2012 Computing in Cardiology*, 245–248. IEEE.
- Vaswani, A.; Shazeer, N.; Parmar, N.; Uszkoreit, J.; Jones, L.; Gomez, A. N.; Kaiser, Ł.; and Polosukhin, I. 2017. Attention is all you need. *Advances in neural information processing systems*, 30.
- Williams, C. K.; and Rasmussen, C. E. 2006. *Gaussian processes for machine learning*. MIT press Cambridge, MA.
- Yadav, P.; Steinbach, M.; Kumar, V.; and Simon, G. 2018. Mining electronic health records (EHRs) A survey. *ACM Computing Surveys (CSUR)*, 50(6): 1–40.
- Zhou, H.; Zhang, S.; Peng, J.; Zhang, S.; Li, J.; Xiong, H.; and Zhang, W. 2021. Informer: Beyond efficient transformer for long sequence time-series forecasting. In *Proceedings of the AAAI Conference on Artificial Intelligence*, volume 35, 11106–11115.



## A Experiments for deterministic interpolation

Although in the current work, we focus on probabilistic interpolation, a reader would be interested in seeing the performance of the model only in the deterministic setting. In Section 4.8, we compare the competing models for deterministic interpolation on the published results. Here, in Table 7, we present the results for all the 5 datasets using the preprocessing steps mentioned in Section D. We observe that Tripletformer provides best performance in 24 out of 30 comparisons making it a promising model for deterministic interpolation as well.

## B Ablation study: Tripletformer vs. Tf-dec-IMAB

Here, we compare the Tripletformer with Tf-dec-IMAB which is a variant of Tripletformer where MAB is replaced with IMAB in the decoder. Comparisons are made using all the datasets for both random and burst sampling. We see that, among 17 out of 30 comparisons Tripletformer performs better than Tf-dec-IMAB. Among real AsTS datasets, Tf-dec-IMAB provides better performance in burst sampling for MIMIC-III with 50% and 90% time points and Physionet2019 in 90% time points in conditioning range. Whereas Tripletformer has better performance in Physionet2012 dataset for both sampling techniques when conditioned up of 50% and 90% of the available time points. We see similar behavior for synthetic AsTS datasets as well. While Tf-dec-IMAB performs better for PenDigits, Tripletformer performs better in PhonemeSpectra. We see that though Tf-dec-IMAB predicts well in some scenarios, on an average Tripletformer provide around 5% less error compared to Tf-dec-IMAB.

## C Datasets

We use the following real world AsTS datasets in the experiments.

**physionet2012:** The PhysioNet Challenge 2012 dataset (Silva et al. 2012; Goldberger et al. 2000) comprises AsTS data extracted from the records of 8,000 patients admitted to ICU. Up to 41 variables were measured for the first 48 hours after the patient’s admission.

**MIMIC-III:** The MIMIC-III dataset (Johnson et al. 2016) also comprises records of ICU patients at Beth Israel Deaconess Medical Center. All the time series contain asynchronous measurements. We follow the procedures of (Horn et al. 2020; Harutyunyan et al. 2019) for splitting the dataset that contains around 21,000 stays with 17 physiological variables being observed.

**Physionet2019:** The Physionet2019 sepsis early prediction challenge dataset (Reyna et al. 2019) was launched for the early detection of sepsis from the clinical data. Dataset consists of the observations collected from patients admitted into intensive care units at three different hospitals in the U.S.A. It consists of around 40,000 samples with 38 variables being observed.

## D Hyperparameters searched for the baseline models

Following hyperparameters are searched for the competing models

**GPR** Following (Shukla and Marlin 2022) we use squared exponential kernel. We search learning rate from  $\{0.1, 0.1, 0.001\}$  and batch size from  $\{32, 64, 128, 256\}$ . In Table 14, we provide best hyperparameters used for GPR.

**ODE models:** We search the standard deviation over the range of  $\{0.01, 0.2, 0.4, 0.6, 0.8, 1.0, 1.2, 1.4, 1.6, 1.8, 2.0\}$ . We select the number of GRU hidden units, latent dimension, nodes in the fully connected network for the ode function in both encoder and decoder from  $\{20, 32, 64, 128, 256\}$ . Number of fully connected layers are searched in the range of  $\{1, 2, 3\}$ . In Tables 12 and 10, we provide best hyperparameters used for L-ODE-ODE and L-ODE-RNN respectively.

**mTAN:** We search the standard deviation from  $\{0.01, 0.2, 0.4, 0.6, 0.8, 1.0, 1.2, 1.4, 1.6, 1.8, 2.0\}$ . We select number of attention heads from  $\{1, 2, 4\}$ , reference points from  $\{8, 16, 32, 64, 128\}$ , latent dimensions from  $\{20, 30, 40, 50\}$ , generator layers from  $\{25, 50, 100, 150\}$ , and reconstruction layers from  $\{32, 64, 128, 256\}$ . We provide best hyperparameters for mTAN in Table 13

**HETVAE:** We search the same hyperparameter range mentioned in (Shukla and Marlin 2022). We set time embedding dimension to 128, search hidden nodes in the decoder from  $\{16, 32, 64, 128\}$ , number reference points from  $\{4, 8, 16, 32\}$ , latent dimension from  $\{8, 16, 32, 64, 128\}$ , width of the fully connected layers from  $\{128, 256, 512\}$  and augmented learning objective from  $\{1.0, 5.0, 10.0\}$ . Best hyperparameters used for HETVAE are provided in Table 11

**Tripletformer:** We search the following hyperparameters:  $L \in \{1, 2, 3, 4\}$ , hidden units in MLP layers (feed forward layers in both encoder and decoder) from  $\{64, 128, 256\}$ , attention layers dimension from  $\{64, 128, 256\}$ , number of induced points in IMAB from  $\{16, 32, 64, 128\}$ , and  $\lambda$  augmented loss weight from  $\{0, 1, 5, 10\}$ . We use softplus activation ( $f(x) = \log(1 + \exp(x))$ ) with a bias of  $10^{-8}$  for outputting the variance of the prediction. The best hyperparameters of Tripletformer are provided in Table 9

We provide the source code of the Tripletformer with instructions in <https://anonymous.4open.science/r/tripletformer-735B>.

### Data preprocessing

We observe that the datasets contain erroneous observations. For example, in Physionet dataset we observe that a few readings in the Ph Value are around 700 which is clearly an error as the Ph value ranges from 0 to 14. Hence, as a standard practice for all the real world AsTS datasets, we consider the observations that are beyond 99.9<sup>th</sup> percentile of the observation range in the training data as anomalies and removed those observations from the entire dataset. We rescale the time between  $[0, 1]$  for all the datasets. We standardize each channel in the series. First we compute the

Table 7: Results for deterministic interpolation on all the datasets. Evaluation measure is Mean Squared Error, lower the best.

tp. obs.	10%	50%	90%	10%	50%	90%
	random missing			burst missing		
	Physionet					
Mean	0.976	0.971	0.963	0.974	0.973	0.984
Forward	0.891	0.655	0.548	1.297	0.958	0.697
GPR	0.586±0.000	0.424±0.002	0.414±0.000	0.708±0.025	0.593±0.002	0.336±0.001
L-ODE-RNN	0.690±0.021	0.618±0.047	0.718±0.058	0.697±0.005	0.922±0.009	0.737±0.023
L-ODE-ODE	0.581±0.001	0.493±0.003	0.497±0.006	0.684±0.000	0.639±0.003	0.644±0.002
mTAN	0.530±0.001	0.377±0.001	0.368±0.002	0.646±0.001	0.569±0.002	0.392±0.001
HETVAE	0.549±0.001	0.378±0.001	0.343±0.002	0.635±0.002	0.567±0.002	<b>0.331±0.001</b>
Tripletformer	<b>0.525±0.006</b>	<b>0.372±0.007</b>	<b>0.331±0.011</b>	<b>0.627±0.001</b>	<b>0.554±0.004</b>	0.335±0.003
	MIMIC-III					
Mean	1.198	1.194	1.210	1.199	1.197	1.199
Forward	1.893	0.984	0.792	2.388	1.436	0.953
GPR	1.055±0.006	0.480±0.010	0.425±0.001	1.164±0.001	0.761±0.005	0.468±0.040
mTAN	0.661±0.001	0.477±0.001	0.474±0.001	0.805±0.001	0.710±0.001	0.511±0.001
HETVAE	0.676±0.001	0.472±0.001	0.430±0.001	0.804±0.002	0.727±0.002	<b>0.446±0.000</b>
Tripletformer	<b>0.646±0.023</b>	<b>0.462±0.017</b>	<b>0.414±0.008</b>	<b>0.788±0.002</b>	<b>0.684±0.001</b>	0.448±0.002
	Physionet2019					
Mean	1.008	1.009	1.008	1.008	1.010	1.004
Forward	0.875	0.642	0.569	1.107	0.916	0.672
GPR	0.611±0.001	0.406±0.002	0.368±0.001	0.765±0.000	0.522±0.000	0.476±0.003
mTAN	<b>0.581±0.002</b>	0.419±0.002	0.415±0.005	0.737±0.001	0.541±0.001	0.461±0.002
HETVAE	0.593±0.000	0.410±0.001	<b>0.350±0.000</b>	0.744±0.005	0.515±0.000	0.485±0.002
Tripletformer	0.585±0.001	<b>0.392±0.001</b>	0.371±0.003	<b>0.591±0.009</b>	<b>0.392±0.001</b>	<b>0.370±0.003</b>
	PenDigits					
Mean	1.010	1.002	0.943	1.017	0.954	0.943
Forward	1.296	1.508	1.425	1.311	1.694	1.425
GPR	1.372±0.004	0.654±0.008	0.462±0.012	1.287±0.002	0.846±0.010	0.462±0.012
L-ODE-RNN	0.729±0.009	0.519±0.024	0.356±0.027	0.701±0.004	0.524±0.010	0.356±0.027
L-ODE-ODE	0.773±0.001	0.515±0.002	0.358±0.013	0.694±0.002	0.568±0.040	0.358±0.013
mTAN	0.783±0.004	0.453±0.007	0.335±0.018	0.743±0.003	0.466±0.005	0.335±0.018
HETVAE	0.814±0.001	0.725±0.019	0.848±0.011	0.736±0.026	0.723±0.001	0.848±0.011
Tripletformer	<b>0.695±0.008</b>	<b>0.326±0.003</b>	<b>0.215±0.016</b>	<b>0.644±0.001</b>	<b>0.408±0.004</b>	<b>0.215±0.016</b>
	PhonemeSpectra					
Mean	1.066	1.060	1.072	1.071	1.048	1.006
Forward	1.360	1.348	1.237	1.419	1.598	1.505
GPR	0.924±0.003	0.793±0.008	0.681±0.011	0.939±0.000	0.839±0.000	0.799±0.000
L-ODE-RNN	0.812±0.013	0.736±0.018	0.680±0.051	0.938±0.019	0.873±0.027	0.777±0.004
L-ODE-ODE	0.768±0.004	0.705±0.012	0.684±0.019	0.894±0.001	0.846±0.004	0.740±0.002
mTAN	0.698±0.005	0.409±0.006	0.515±0.016	0.896±0.001	<b>0.782±0.002</b>	0.817±0.011
HETVAE	0.785±0.002	0.385±0.010	0.528±0.004	0.887±0.001	0.815±0.001	<b>0.808±0.002</b>
Tripletformer	<b>0.679±0.011</b>	<b>0.367±0.035</b>	<b>0.210±0.009</b>	<b>0.854±0.001</b>	0.808±0.001	0.796±0.002

Table 8: Comparing Tripletformer and Tf-dec-IMAB. Tf-enc-MAB is a variant of Tripletformer and consists of the IMAB in the decoder instead of the MAB. Results of synthetic AsTS. Evaluation measure is NLL, lower the best.

tp. obs.	10%		50%		90%	
	Tripletformer	Tf-dec-IMAB	Tripletformer	Tf-dec-IMAB	Tripletformer	Tf-dec-IMAB
random sampling						
Physionet2012	<b>0.780±0.013</b>	0.845±0.015	<b>0.455±0.011</b>	0.565±0.05	<b>0.373±0.040</b>	0.703±0.092
MIMIC-III	1.056±0.006	<b>1.053±0.037</b>	0.789±0.006	<b>0.783±0.01</b>	<b>0.710±0.010</b>	0.735±0.018
Physionet2019	1.079±0.001	<b>1.061±0.003</b>	0.806±0.004	<b>0.796±0.002</b>	<b>0.752±0.007</b>	0.797±0.017
PenDigits	1.115±0.003	<b>1.113±0.001</b>	<b>0.693±0.019</b>	0.717±0.028	0.463±0.027	<b>0.386±0.054</b>
PhonemeSpectra	<b>0.923±0.008</b>	0.951±0.009	<b>0.413±0.005</b>	0.570±0.174	<b>0.115±0.024</b>	0.250±0.042
bursts sampling						
Physionet2012	<b>0.925±0.005</b>	0.946±0.007	<b>0.777±0.013</b>	0.821±0.008	<b>0.578±0.034</b>	0.794±0.023
MIMIC-III	<b>1.193±0.003</b>	1.203±0.003	1.087±0.006	<b>1.023±0.006</b>	0.885±0.032	<b>0.835±0.015</b>
Physionet2019	1.222±0.001	<b>1.210±0.001</b>	<b>0.977±0.005</b>	0.980±0.003	0.865±0.009	0.785±0.009
PenDigits	<b>1.115±0.000</b>	1.127±0.001	0.787±0.015	<b>0.735±0.015</b>	0.463±0.027	<b>0.386±0.054</b>
PhonemeSpectra	<b>1.180±0.008</b>	1.217±0.007	<b>1.025±0.005</b>	1.032±0.011	0.975±0.009	<b>0.950±0.011</b>

mean and standard deviation of all the observations present in a channel; and for each observation measurement, we subtract mean and divide the residual with the standard deviation.

Table 9: Best hyperparameters used in Tripletformer

dataset	Samp. Type	Obs. %	batch size	lr	mse wt	IMAB dim	CAB dim	dec. dim	nlayers	#ref-points
Phys.2012	random	0.1	128	0.001	1	64	256	128	1	128
Phys.2012	random	0.5	128	0.001	1	128	126	64	4	32
Phys.2012	random	0.9	128	0.001	5	256	256	256	3	128
Phys.2012	bursts	0.1	128	0.001	5	128	256	64	3	32
Phys.2012	bursts	0.5	128	0.001	10	128	256	128	3	128
Phys.2012	bursts	0.9	128	0.001	10	128	256	128	2	32
mimiciiii	random	0.1	128	0.001	10	256	256	64	3	16
mimiciiii	random	0.5	128	0.001	0	128	256	256	1	128
mimiciiii	random	0.9	128	0.001	1	64	256	256	4	16
mimiciiii	bursts	0.1	128	0.001	0	128	256	256	1	32
mimiciiii	bursts	0.5	128	0.001	5	128	128	256	4	64
mimiciiii	bursts	0.9	128	0.001	10	256	256	128	4	128
Phys.2019	random	0.1	64	0.001	0	128	64	256	3	128
Phys.2019	random	0.5	64	0.001	5	128	128	256	4	16
Phys.2019	random	0.9	64	0.001	1	128	128	128	1	128
Phys.2019	bursts	0.1	64	0.001	0	128	128	128	2	32
Phys.2019	bursts	0.5	64	0.001	0	64	128	256	3	16
Phys.2019	bursts	0.9	64	0.001	1	128	64	256	4	16
PenDigits	random	0.1	128	0.001	1	128	128	128	3	128
PenDigits	random	0.5	128	0.001	10	128	128	128	4	16
PenDigits	random	0.9	128	0.001	0	64	256	64	2	16
PenDigits	bursts	0.1	128	0.001	10	64	256	64	3	64
PenDigits	bursts	0.5	128	0.001	0	256	256	128	4	16
Phon.Spec.	random	0.1	128	0.001	5	256	64	256	4	16
Phon.Spec.	random	0.5	128	0.001	5	64	256	64	4	16
Phon.Spec.	random	0.9	128	0.001	5	128	256	256	2	64
Phon.Spec.	bursts	0.1	128	0.001	10	64	128	256	1	16
Phon.Spec.	bursts	0.5	128	0.001	5	256	64	256	3	64
Phon.Spec.	bursts	0.9	128	0.001	0	64	256	128	1	32

Table 10: Best hyperparameters used for L-ODE-RNN

Dataset	Sampling Type	Obs. %	batch size	lr	rec dims	gru units	units	gen layers	rec layers	z0 encoder
Phys.2012	random	10	64	0.0001	64	32	256	1	1	rmn
Phys.2012	random	50	64	0.0001	256	256	64	1	2	rmn
Phys.2012	random	90	64	0.0001	64	128	256	1	2	rmn
Phys.2012	burst	10	64	0.0001	256	20	20	1	3	rmn
Phys.2012	burst	50	64	0.0001	32	256	64	3	2	rmn
Phys.2012	burst	90	64	0.0001	256	64	32	2	3	rmn
PenDigits	random	10	64	0.0001	128	20	256	3	2	rmn
PenDigits	random	50	64	0.0001	256	32	64	3	1	rmn
PenDigits	random	90	64	0.0001	256	256	128	1	1	rmn
PenDigits	burst	10	64	0.0001	256	64	256	1	3	rmn
PenDigits	burst	50	64	0.0001	128	64	256	1	3	rmn
PenDigits	burst	90	64	0.0001	128	32	64	2	3	rmn
Phon.Spec.	random	10	64	0.0001	256	20	128	1	3	rmn
Phon.Spec.	random	50	64	0.0001	256	20	128	2	1	rmn
Phon.Spec.	random	90	64	0.0001	256	128	256	1	3	rmn
Phon.Spec.	burst	10	64	0.0001	64	128	256	2	3	rmn
Phon.Spec.	burst	50	64	0.0001	32	64	256	2	3	rmn
Phon.Spec.	burst	90	64	0.0001	64	20	256	1	1	rmn

Table 11: Best hyperparameters of HETVAE model

Dataset	Samp. Type	Obs. %	learn. rate	batch size	rec hid.	latent dim	width	embed time	#ref points	mse wt.
Phys.2012	random	10	0.0001	128	128	128	128	128	16	5
Phys.2012	random	50	0.0001	128	128	64	512	128	8	1
Phys.2012	random	90	0.0001	128	32	128	128	128	32	5
Phys.2012	burst	10	0.0001	128	64	128	128	128	32	1
Phys.2012	burst	50	0.0001	128	64	128	512	128	16	10
Phys.2012	burst	90	0.0001	128	128	128	256	128	16	1
MIMIC-III	random	10	0.0001	128	128	64	512	128	32	10
MIMIC-III	random	50	0.0001	128	64	64	256	128	8	5
MIMIC-III	random	90	0.0001	128	16	128	512	128	32	5
MIMIC-III	burst	10	0.0001	128	64	128	256	128	32	1
MIMIC-III	burst	50	0.0001	128	32	64	256	128	16	10
MIMIC-III	burst	90	0.0001	128	32	128	128	128	4	1
Phys.2019	random	10	0.0001	128	64	32	512	128	16	5
Phys.2019	random	50	0.0001	128	32	128	128	128	32	1
Phys.2019	random	90	0.0001	128	16	32	256	128	32	10
Phys.2019	burst	10	0.0001	128	64	16	128	128	32	5
Phys.2019	burst	50	0.0001	128	128	128	128	128	32	1
Phys.2019	burst	90	0.0001	128	128	16	128	128	32	1
PenDigits	random	10	0.0001	128	16	128	128	128	8	1
PenDigits	random	50	0.0001	128	16	32	512	128	16	5
PenDigits	random	90	0.0001	128	32	64	128	128	4	5
PenDigits	burst	10	0.0001	128	64	32	512	128	8	10
PenDigits	burst	50	0.0001	128	64	64	512	128	32	5
PenDigits	burst	90	0.0001	128	32	8	512	128	16	10
Phon.Spec.	random	10	0.0001	128	128	32	256	128	16	10
Phon.Spec.	random	50	0.0001	128	128	128	512	128	16	10
Phon.Spec.	random	90	0.0001	128	16	64	512	128	8	1
Phon.Spec.	burst	10	0.0001	128	32	8	128	128	8	1
Phon.Spec.	burst	50	0.0001	128	32	8	128	128	8	1
Phon.Spec.	burst	90	0.0001	128	64	8	512	128	32	1

Table 12: Best hyperparameters used in L-ODE-ODE

Dataset	Sampling Type	Obs. %	batch size	lr	rec dims	gru units	units	gen layers	rec layers	rec hidden
Phys.2012	random	10	64	0.0001	32	128	32	1	1	128
Phys.2012	random	50	64	0.0001	256	32	128	2	3	64
Phys.2012	random	90	64	0.0001	32	256	64	3	3	64
Phys.2012	burst	10	64	0.0001	64	256	64	2	1	16
Phys.2012	burst	50	64	0.0001	20	32	64	1	1	128
Phys.2012	burst	90	64	0.0001	128	32	32	3	2	128
PenDigits	random	10	64	0.0001	256	32	256	2	3	32
PenDigits	random	50	64	0.0001	32	64	128	1	3	128
PenDigits	random	90	64	0.0001	64	256	128	2	1	16
PenDigits	burst	10	64	0.0001	32	256	128	2	2	32
PenDigits	burst	50	64	0.0001	64	256	256	3	3	128
PenDigits	burst	90	64	0.0001	64	256	128	1	2	16
Phon.Spec.	random	10	64	0.0001	64	64	256	1	2	128
Phon.Spec.	random	50	64	0.0001	128	32	128	3	2	64
Phon.Spec.	random	90	64	0.0001	32	128	256	1	1	64
Phon.Spec.	burst	10	64	0.0001	128	20	128	3	2	16
Phon.Spec.	burst	50	64	0.0001	32	256	64	1	1	16
Phon.Spec.	burst	90	64	0.0001	64	20	32	1	3	64

Table 13: Best hyperparameters for mTAN model

Dataset	Samp. Type	Obs. %	batch size	embed time	gen hid.	latent dim	lr	#ref points	rec hid.
Phys.2012	random	10	128	128	128	32	0.001	8	128
Phys.2012	random	50	128	128	128	128	0.001	16	64
Phys.2012	random	90	128	128	32	128	0.001	8	64
Phys.2012	burst	10	128	128	16	64	0.001	16	16
Phys.2012	burst	50	128	128	128	64	0.001	16	128
Phys.2012	burst	90	128	128	64	32	0.001	8	128
MIMIC-III	random	10	128	128	32	8	0.001	16	128
MIMIC-III	random	50	128	128	64	16	0.001	8	128
MIMIC-III	random	90	128	128	128	8	0.001	8	16
MIMIC-III	burst	10	128	128	128	16	0.001	16	64
MIMIC-III	burst	50	128	128	128	16	0.001	16	32
MIMIC-III	burst	90	128	128	128	64	0.001	4	128
Phys.2019	random	10	128	128	32	128	0.001	32	128
Phys.2019	random	50	128	128	64	16	0.001	16	16
Phys.2019	random	90	128	128	64	16	0.001	32	64
Phys.2019	burst	10	128	128	32	16	0.001	16	32
Phys.2019	burst	50	128	128	128	32	0.001	32	32
Phys.2019	burst	90	128	128	128	64	0.001	8	128
PenDigits	random	10	128	128	128	128	0.001	16	32
PenDigits	random	50	128	128	32	32	0.001	16	128
PenDigits	random	90	128	128	128	64	0.001	32	16
PenDigits	burst	10	128	128	128	16	0.001	16	32
PenDigits	burst	50	128	128	32	8	0.001	16	128
PenDigits	burst	90	128	128	128	8	0.001	8	16
Phon.Spec.	random	10	128	128	16	32	0.001	16	128
Phon.Spec.	random	50	128	128	64	8	0.001	32	64
Phon.Spec.	random	90	128	128	32	64	0.001	32	64
Phon.Spec.	burst	10	128	128	128	16	0.001	16	16
Phon.Spec.	burst	50	128	128	32	32	0.001	32	16
Phon.Spec.	burst	90	128	128	16	8	0.001	16	64



Table 14: Best hyperparameters used for GPR

dataset	Samp. Type	Obs. %	batch size	lr
Phys.2012	random	0.1	64	0.01
Phys.2012	random	0.5	32	0.01
Phys.2012	random	0.9	32	0.001
Phys.2012	bursts	0.1	128	0.01
Phys.2012	bursts	0.5	128	0.001
Phys.2012	bursts	0.9	32	0.01
mimiciii	random	0.1	64	0.001
mimiciii	random	0.5	32	0.001
mimiciii	random	0.9	32	0.01
mimiciii	bursts	0.1	32	0.01
mimiciii	bursts	0.5	128	0.001
mimiciii	bursts	0.9	32	0.0001
Phys.2019	random	0.1	64	0.001
Phys.2019	random	0.5	32	0.01
Phys.2019	random	0.9	32	0.001
Phys.2019	bursts	0.1	128	0.001
Phys.2019	bursts	0.5	32	0.001
Phys.2019	bursts	0.9	32	0.0001
PenDigits	random	0.1	64	0.001
PenDigits	random	0.5	128	0.001
PenDigits	random	0.9	32	0.0001
PenDigits	bursts	0.1	32	0.01
PenDigits	bursts	0.5	32	0.001
PenDigits	bursts	0.9	32	0.0001
Phon.Spec.	random	0.1	32	0.001
Phon.Spec.	random	0.5	64	0.01
Phon.Spec.	random	0.9	32	0.001
Phon.Spec.	bursts	0.1	32	0.01
Phon.Spec.	bursts	0.5	64	0.01
Phon.Spec.	bursts	0.9	32	0.01